

ARTICLE

Received 22 Jul 2015 | Accepted 2 Sep 2016 | Published 7 Oct 2016

DOI: 10.1038/ncomms13101

OPEN

Endoglin integrates BMP and Wnt signalling to induce haematopoiesis through JDP2

June Baik¹, Alessandro Magli¹, Naoyuki Tahara^{2,3}, Scott A. Swanson⁴, Naoko Koyano-Nakagawa¹, Luciene Borges¹, Ron Stewart⁴, Daniel J. Garry¹, Yasuhiko Kawakami^{2,3}, James A. Thomson⁴ & Rita C.R. Perlingeiro¹

Mechanisms of haematopoietic and cardiac patterning remain poorly understood. Here we show that the BMP and Wnt signalling pathways are integrated in an endoglin (Eng)-dependent manner in cardiac and haematopoietic lineage specification. Eng is expressed in early mesoderm and marks both haematopoietic and cardiac progenitors. In the absence of Eng, yolk sacs inappropriately express the cardiac marker, Nkx2.5. Conversely, high levels of Eng *in vitro* and *in vivo* increase haematopoiesis and inhibit cardiogenesis. Levels of Eng determine the activation of both BMP and Wnt pathways, which are integrated downstream of Eng by phosphorylation of Smad1 by Gsk3. By interrogating Eng-dependent Wnt-mediated transcriptional changes, we identify *Jdp2* as a key Eng-dependent Wnt target, sufficient to establish haematopoietic fate in early mesoderm when BMP and Wnt crosstalk is disturbed. These studies provide mechanistic insight into the integration of BMP and Wnt signalling in the establishment of haematopoietic and cardiac progenitors during embryogenesis.

¹ Department of Medicine, Lillehei Heart Institute, University of Minnesota, Minneapolis, Minnesota 55455, USA. ² Department of Genetics, Cell Biology, and Development, University of Minnesota, Minneapolis, Minnesota 55455, USA. ³ Stem Cell Institute, University of Minnesota, Minneapolis, Minnesota 55455, USA. ⁴ Regenerative Biology, Morgridge Institute for Research, Madison, Wisconsin 53715, USA. Correspondence and requests for materials should be addressed to R.C.R.P. (email: perli032@umn.edu).

In the developing embryos, haematopoietic and cardiac cells arise as subpopulations of lateral plate mesoderm^{1,2}, but the phenotypic profiles of these progenitors as well as the molecular mechanisms regulating their specification remain not well defined. It is known that BMP and Wnt signals from the extra-embryonic region and epiblast, respectively, are required for mesoderm induction³. Homozygous deletion of BMP4 and its type 1 receptor BMPR1a, as well as Wnt3 and its intercellular effector β -catenin, result in embryonic lethality due to the failure of mesoderm formation and subsequent patterning. Wnt signals along with BMP are also critical to establish the prospective cardiac population¹ by directing the migration of cardiac progenitors from the primitive streak to the heart forming region⁴. This convergence of Wnt and BMP signalling is also observed during haematopoiesis. Studies involving avian embryo manipulation and *in vitro* differentiation of murine embryonic stem (ES) cells have demonstrated that the combination of Wnt and BMP signalling is essential for haematopoietic specification and commitment towards the primitive erythroid lineage^{1,5,6}.

We previously reported that endoglin (Eng), an ancillary receptor for the transforming growth factor- β superfamily, is required for early haematopoietic lineage specification, and that Eng acts by modulating output of the BMP signalling pathway⁷⁻⁹. Haematopoiesis was found impaired in both Eng-deficient differentiating ES cells¹⁰ and embryos⁹. On the other hand, upregulation of Eng using doxycycline-inducible Eng (iEng) ES cells resulted in enhanced haematopoietic differentiation and suppressed cardiac differentiation⁷, suggesting a key role for this receptor in early cell fate specification.

Using zebrafish and mouse models, in the present study, we provide *in vivo* evidence for the dual role of Eng in blood and cardiac lineage specification, and show that this effect results from enhanced Wnt activity, which is directly regulated by Eng. In fact, levels of Eng determine the activation potential of both BMP and Wnt pathways, and phosphorylation of Smad1 by Gsk3 is the point of integration between BMP and Wnt signals. We further show that Eng identifies early progenitors endowed with haematopoietic and cardiac potential that are Eng⁺Flk-1⁺ and Eng⁺Flk-1⁻, respectively, demonstrating that Eng marks not only haematopoietic but also cardiac cell fate within the mesoderm population. Through whole transcriptome analyses of these early haematopoietic and cardiac progenitor fractions, in the presence or absence of the Wnt inhibitor IWR, we identified *Jdp2*, a member of the AP-1 transcription factor family, as a key Eng-dependent downstream target of Wnt signalling. Importantly, we show *Jdp2* expression is sufficient to establish haematopoietic fate in early mesoderm when BMP and Wnt crosstalk is disturbed, providing mechanistic insight into the establishment of haematopoietic and cardiac progenitors during embryogenesis.

Results

Effect of Eng induction *in vitro* and *in vivo*. Our previous findings using *in vitro* differentiation of iEng ES cells suggest a time-dependent effect, as Eng overexpression from day 2 to 8 of embryoid body (EB) differentiation repressed cardiogenesis, whereas Eng overexpression from day 4 to 8 had no effect⁷. To better understand this temporal dependence, we performed a fine time-course analysis, which revealed a short window from day 2 to 3 in which overexpression of Eng enhances haematopoiesis and represses cardiac differentiation (Supplementary Fig. 1a,b). This is the time at which mesoderm is being specified to haematopoietic or cardiac fate. To investigate whether Eng induction results in cardiac suppression *in vivo*, we collected E8.5 mouse embryos, a time point with abundant cardiovascular progenitors¹¹, and

transduced these with lentiviral vectors encoding Eng or empty vector (control pSAM; Supplementary Fig. 1c). Control explant cultures gave rise to large clusters of cells positive for cTnI (Supplementary Fig. 1d, lower left), in contrast to Eng-transduced explants, which presented significantly reduced numbers of cells expressing cTnI (Supplementary Fig. 1d, lower right). In a complementary approach, we utilized a cardiac reporter transgenic zebrafish, in which GFP identifies cardiac progenitors that are positive for myosin light chain 2 *Tg(cmlc2:EGFP)*¹², to determine whether Eng induction disturbs cardiac specification *in vivo*. For this, *Tg(cmlc2:EGFP)* embryos at the 1–2-cell stage were injected with human *ENG* messenger RNA (mRNA), which has been previously demonstrated to cross-react in zebrafish¹³, or with control *mCherry* mRNA. Consistent with our *in vitro* and *ex vivo* studies, live imaging analyses at 16 h post fertilization (h.p.f.) demonstrated impaired cardiogenesis in *ENG*-injected embryos, evidenced by reduced levels of GFP expression (Fig. 1a, right panel) when compared with *mCherry*-injected controls (Fig. 1a, left panel). Fluorescence-activated cell sorting (FACS) analyses confirmed that the number of EGFP⁺ (*cmlc2*⁺) cells within the *ENG*⁺ population was reduced when compared with those within the control *mCherry*⁺ population (Fig. 1b), further indicating that enhanced expression of Eng represses cardiac specification during gastrulation.

To further evaluate the activity of Eng in cardiac versus haematopoietic specification, we utilized a potent hemogenic tissue, E9.5 yolk sac (YS). *Eng*^{-/-} E9.5 YSs have been reported to exhibit severely reduced haematopoietic colony activity as well as marked downregulation of *Scl*, *Gata1*, *Gata2* and globins⁹. Thus, we interrogated here whether the role of Eng was to actively repress other lineages in E9.5 YSs (Supplementary Fig. 1e). At the gene expression level, we observed significant upregulation of *Nkx2.5* (Supplementary Fig. 1f, left), one of the earliest markers of cardiac development¹⁴. Expression levels of *Gata4* and *cTnI* also trended towards elevated levels in *Eng*-null YSs (Supplementary Fig. 1f). These data suggest a role for Eng in enabling the haematopoietic program by preventing the expression of cardiac-specific genes at hemogenic sites during mesoderm specification.

We then evaluated the effect of overexpressing Eng *in vivo* during mouse embryo development using iEng mice, which we generated from the previously described iEng ES cells⁷. As observed in Fig. 1c, robust induction of Eng was observed in E8.5 YSs from embryos whose mothers were treated with dox during pregnancy. Next, equal numbers of YS cells from these embryos were directly plated into methylcellulose containing haematopoietic cytokines to examine haematopoietic colony activity. As observed in Fig. 1d, Eng-induced YSs gave rise to increased numbers of haematopoietic colonies when compared with non-induced YSs, confirming that Eng induction results in enhanced haematopoiesis. To assess cardiogenesis, we dissected E8.5 embryos, and separated anterior (containing cardiac progenitors) from posterior domains (used for genotype). Expression of *Pdgfra* and Flk-1 identifies cardiac progenitors at this developmental stage^{15,16}, therefore we analysed the expression of these markers in the Eng⁺ cell fraction of the anterior regions of these embryos. In agreement with our hypothesis, the frequency of *Pdgfra*⁺Flk-1⁺ cells within the Eng⁺ population was found significantly decreased when Eng was induced (Fig. 1e,f). Taken together, these *in vivo* data confirm dual positive/negative functions for Eng in the establishment of haematopoietic and cardiac progenitors, respectively, during mesoderm specification.

Eng directly regulates Wnt signalling. Based on the critical role of Wnt signalling during early haematopoiesis and

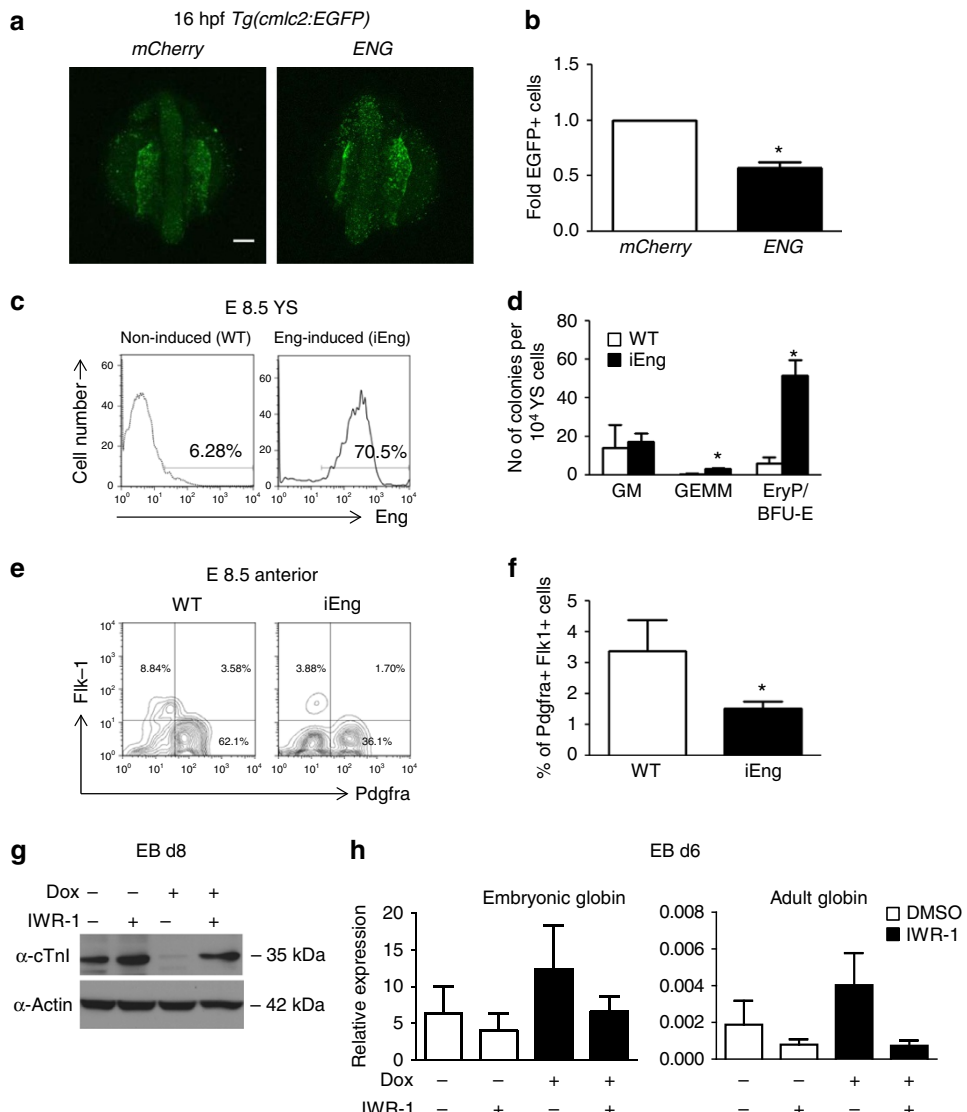


Figure 1 | The dual effect of endoglin in early cell specification requires Wnt activation. (a,b) ENDOGLIN (ENG) and control *mCherry* mRNAs were injected into *Tg(cmlc2:EGFP)* zebrafish embryos. (a) Embryos were imaged to visualize cardiac progenitors (EGFP⁺ cells) at 16 h.p.f. All views are dorsal. Scale bar, 100 μ m. (b) Graph bars show the fold difference of EGFP⁺ cells, quantified by FACS, between ENG- and *mCherry*-injected embryos, which show reduced frequency of cardiac progenitors upon ENG induction. Bars represent s.e.m. from three independent experiments. * $P < 0.05$ by *t*-test. (c-f) YSs and anterior regions of E8.5 endoglin-induced mouse embryos were collected and analysed for haematopoietic and cardiac potential, respectively. (c) FACS analyses show induction of endoglin expression in the yolk sac of E8.5 iEng mice (right panel). (d) YSs from Eng-induced and control (WT) counterparts were assessed for their haematopoietic activity. Significant increased numbers of erythroid and GEMM colonies were observed upon endoglin induction. Error bars indicate s.e.m. from two litters of E8.5 Eng-induced ($n = 13$) and WT littermate control ($n = 4$) YSs. * $P < 0.05$ by *t*-test. (e) Representative FACS profiles for the expression of *Pdgfra* and *Flk-1* in the anterior regions of E8.5 endoglin-induced mouse embryos and control (WT) counterparts. (f) Quantification of *Pdgfra*⁺ *Flk-1*⁺ cells confirms cardiac suppression upon induction of endoglin. Bars indicate s.e.'s from two litters of E8.5 Eng-induced ($n = 13$) and WT littermate control ($n = 4$) embryos. * $P < 0.05$ by *t*-test. (g,h) iEng ES cells were differentiated as EBs. Dox was added to EB cultures from day 2, and IWR-1 from day 4 to 6. EB cultures were analysed for cardiac and haematopoietic differentiation at days 8 and 6, respectively. (g) Western blot analyses reveal rescue of cTnI expression in Eng-induced EBs that had been treated with IWR-1. (h) Gene expression analysis for embryonic and adult globins demonstrates that IWR-1 counteracts the stimulatory effect of endoglin in erythropoiesis. Transcript levels are normalized to *Gapdh*. Bars indicate s.e.'s from three independent experiments.

cardiogenesis^{1,6,17}, we investigated whether Wnt activation is involved in Eng-mediated mesoderm specification. For this, we assessed the effect of the canonical Wnt signalling inhibitor, IWR-1, in Eng-induced EB cultures, and found that the inhibitory effect of Eng induction (+ dox) on cardiac differentiation was abrogated by inhibition of the canonical Wnt signalling pathway (Fig. 1g). To determine whether this would also be the case *in vivo*, we cultured Eng- and mock-transduced embryo explants in the presence or absence of IWR-1. In agreement with the

in vitro EB data, addition of IWR-1 to Eng-transduced primary cultures counteracted the inhibitory effect of Eng on cardiac differentiation (Supplementary Fig. 1g,h). We also observed that Wnt inhibition by IWR-1 in EB cultures negatively affected the ability of Eng to induce haematopoiesis (Fig. 1h), demonstrating that the function of Eng at this early stage of development requires active Wnt signalling.

To determine whether Eng induction promotes Wnt activation, we generated a β -catenin-dependent reporter ES cell line. This

reporter (7xTcf-FFluc//SV40-mCherry) contains 7Tcf-binding sites, allowing us to monitor Wnt activity using a luciferase reporter assay¹⁸. We subjected Eng-induced or control cultures to a brief pulse of Wnt signal (3 h of exposure to the GSK3 β inhibitor CHIR99021), and observed that reporter activity was increased in Eng-induced cultures when compared with non-induced or mock cultures (DMSO treated; Fig. 2a). The increased reporter activity observed in the Eng-induced sample that had been treated with CHIR99021 was confirmed by western blot using an antibody specific for active β -catenin (Fig. 2b). This finding was further corroborated *in vivo* utilizing *Tg(7xTCF:mCherry)* zebrafish embryos, which at 12 h.p.f. exhibit transgenic reporter expression regulated by Wnt/ β -catenin signalling, as measured by mCherry fluorescence¹⁹. We injected 1–2-cell stage zebrafish embryos with *ENG* mRNA or control *venus* mRNA (Fig. 2c, upper panels), and at 12 h.p.f., injected embryos were collected and analysed for mCherry expression. We observed that mCherry expression within the *ENG*⁺ cell fraction in *ENG*-injected embryos was significantly increased when compared with that found within the *venus*⁺ cell fraction in *venus*-injected controls (Fig. 2c, lower panels; Fig. 2d). As expected, mCherry expression within the *ENG*⁻ cell fraction of *ENG*-injected embryos was similar to control levels, ~21% (Supplementary Fig. 2a). Moreover, equivalent results were obtained when we injected an *ENG* mutant construct encoding a deletion of the orphan domain (OD; Supplementary Fig. 2b,c), which is required for *ENG* expression and ligand binding²⁰. Taken together, these data confirm that Eng induction enhances Wnt activity.

The stimulatory effect of Eng in haematopoiesis was previously shown to involve BMP signalling, as evidenced by the decreased frequency of haematopoietic activity correlating with reduced levels of Smad1/5/8 phosphorylation when dorsomorphin, a BMP signalling inhibitor, was added to these cultures⁷. It has been shown in *Xenopus* that Smad1, the downstream effector of BMP signalling, is also a target of Gsk3-mediated phosphorylation²¹. Gsk3 is a component of the Wnt degradation complex, and inhibition of this kinase, which maintains the Wnt pathway active, contributes to the stabilization of activated Smad1 and ultimately strengthens BMP signalling²¹. Consistent with this, western blot analyses of day 4 Eng-induced EB cultures revealed that increased levels of phosphorylated Smad1 (S456/8 and S426/8) were accompanied by higher levels of dephosphorylated active β -catenin and inhibitory forms of Gsk3 (pGsk3 α / β S21/9) (Supplementary Fig. 2d). To determine whether Eng regulates both BMP and Wnt signals to enhance Smad1 activity and, consequently, increased haematopoietic commitment from mesoderm, we investigated whether sustained Wnt-deregulated Smad1 activity could phenocopy Eng overexpression. We generated an ES cell line with inducible expression of mutant Smad1 (S210A) lacking the Gsk3-mediated phosphorylation site (Supplementary Fig. 2e,f), which has been shown to be responsible for Smad1 degradation²¹. As hypothesized, enhanced haematopoiesis was observed only in Smad1 S210A dox-induced cultures (Fig. 2e, left), similar to the effect of Eng induction in this developmental stage⁷. Induction of wild-type (WT) Smad1 had no effect on colony formation. Importantly, whereas Wnt stimulation with CHIR resulted in enhanced haematopoiesis in induced WT Smad1 cultures (iSmad1 WT), no effect was observed in the S210A mutant (Fig. 2e, right), confirming that Wnt-mediated enhancement of haematopoiesis is dependent on the phosphorylation of Smad1 at S210.

To gain further insight into how integration of BMP and Wnt pathways regulates the commitment of mesoderm, we performed chromatin immunoprecipitation in D4 EBs followed by high-throughput sequencing (ChIP-seq) for Smad1 in the absence or

presence of IWR-1. In agreement with the previous reports²², Smad1 binding was detected at the regulatory elements of known BMP targets *Id1*, *Id2* and *Id3* (Fig. 2f), which was also validated by ChIP-quantitative PCR (qPCR; Fig. 2g). Importantly, IWR-1 treatment negatively affected Smad1 binding at specific loci (Fig. 2f,g) and genome wide (Fig. 2h; Supplementary Fig. 2i). Among the 10,466 sites identified, Smad1 binding was impaired at ~3,500 sites and disrupted at ~6,500 sites (respectively, groups A and B—Supplementary Fig. 2i), thus supporting the essential role of BMP and Wnt integration to regulate Smad1 activity at the genome-wide level. Interestingly, we also observed Smad1 binding at *Tbx5* and Wnt inhibitory factor 1 (*Wif1*; Supplementary Fig. 2g,h). *Tbx5*, along with *Nkx2.5*, is a key transcription factor for cardiac specification, as well evidenced by studies showing that disruption of its interaction with chromatin remodelling complex resulted in impaired cardiogenesis²³. Considering that BMP and Wnt integration is critical for cardiac commitment, our data suggest that BMP may repress *Tbx5* expression in mesodermal cells, which could account for Eng-mediated cardiac repression. *Wif1* has been identified as a Smad1 target and it has been postulated to modulate BMP and Wnt activities in the developing mouse lung²⁴. In agreement with Xu and colleagues, we observed that Smad1 occupies similar regions in the promoter and first intron of the *Wif1* gene (Supplementary Fig. 2g). Taken together, these data demonstrate that BMP and Wnt modulation is critical not only for Smad1 stability but also for the genome-wide occupancy of its binding sites in mesodermal cells.

Haematopoietic and cardiac progenitors express Eng. To determine whether Eng expression regulates haematopoietic and cardiac cell fate specification from uncommitted mesodermal progenitors, we utilized a GFP-Brachyury (Bry) reporter ES cell line²⁵. In this cell line, GFP is knocked into the *Bry* locus, allowing us to monitor Bry expression during EB differentiation, and, importantly, to isolate early mesodermal cells. Accordingly, using this reporter ES cell line, Keller and colleagues have demonstrated that in day 3 EBs, haematopoietic progenitors are enriched within the *Bry*⁺ *Flk-1*⁺ cell fraction, whereas cardiac cells are predominantly in the *Bry*⁺ *Flk-1*⁻ cell subpopulation^{11,25}. Based on this evidence, we investigated the expression of endoglin (Eng or E) in combination with Flk-1 (F) in day 3 *Bry*⁺ EB cells. As shown in Fig. 3a, four distinct cell subpopulations were identified: *E*⁺*F*⁺, *E*⁺*F*⁻, *E*⁻*F*⁺ and *E*⁻*F*⁻. These subfractions were FACS-purified, and sorted cells were reaggregated for 24 h in the absence or presence of IWR-1 to determine whether Wnt activity would affect Eng-mediated mesoderm specification. We examined the haematopoietic potential in reaggregates from *E*⁺*F*⁺ and *E*⁻*F*⁺ subpopulations by plating these in methylcellulose containing haematopoietic cytokines. Our results showed a significant enrichment in haematopoietic activity in the *Bry*⁺ cell fraction that is double positive for Eng and Flk-1 (*E*⁺*F*⁺) when compared with the unsorted group (30-fold), and remarkably also superior than the *E*⁻*F*⁺ subpopulation (2-fold) (Fig. 3b, white bars). This enrichment was abrogated by IWR-1, indicating that Wnt activity is required for the haematopoietic commitment of *E*⁺*F*⁺ cells (Fig. 3b, black bars). The inhibitory effect was not observed in cells negative for Eng (*E*⁻*F*⁺; Fig. 3b). Consistent with the previous data²⁵, only very few haematopoietic colonies were observed when the Flk-1-negative cell population was assayed (*E*⁺*F*⁻ and *E*⁻*F*⁻; Supplementary Fig. 3a). To determine their cardiac potential, reaggregates from *E*⁺*F*⁻ and *E*⁻*F*⁻ populations were plated as monolayers in the presence IWR-1. Remarkably, contractile cardiomyocytes were observed

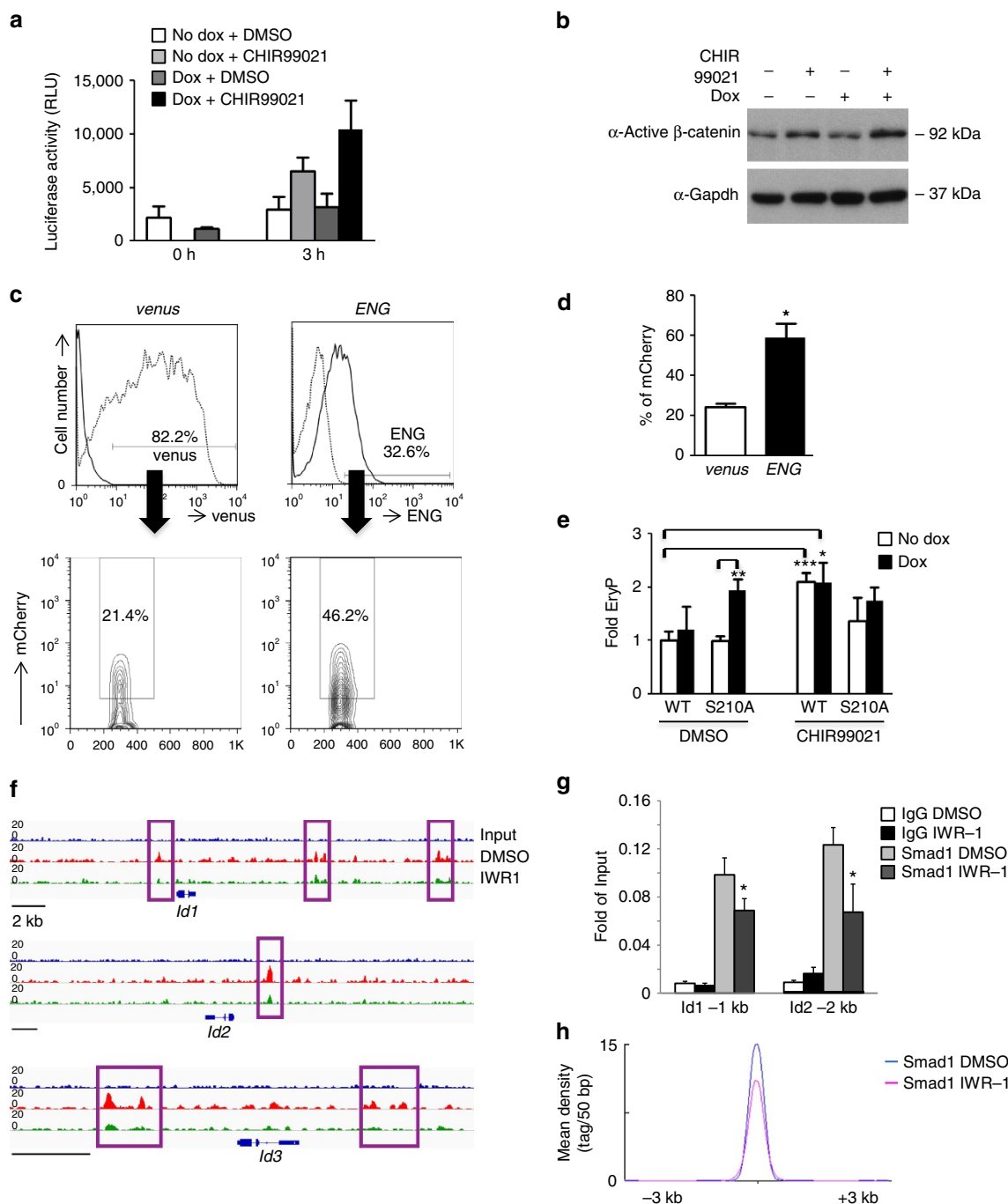


Figure 2 | Endoglin-mediated Wnt activation enhances Smad1 activity to promote hematopoiesis. (a,b) A β -catenin-dependent reporter (7TFC) was introduced into the iEng ES cell line (7TFC:iEng). 7TFC:iEng ES cells were differentiated as EBs, and dox was added to the culture medium from day 2. The GSK3 β -inhibitor CHIR99021 was added to cultures 24 h later, and samples were collected at 0 and 3 h. (a) Luciferase activity denotes Wnt stimulation in these cultures, and peak is observed after 3 h solely in endoglin-induced EB samples that had been exposed to CHIR99021. Graph is representative of three independent experiments. (b) Respective western blot analyses for active β -catenin in EB cultures following 3 h of Wnt stimulation. Consistently, higher levels of active β -catenin are observed in cultures that had been exposed to dox (iEng) and CHIR99021. Gapdh was used as loading control. (c,d) ENG and control venus mRNAs were injected into *Tg(7xTCF:mCherry)* zebrafish embryos. (c) Representative FACS profiles for mCherry expression in micro-injected embryos. mCherry expression from *venus*- and *ENG*-injected groups were gated in either *venus*- or *ENG*-positive cells, respectively. (d) Quantification of mCherry $^{+}$ cells confirms enhanced Wnt activity upon ENG overexpression. Bars represent s.e.m. from three independent experiments. * $P < 0.05$ by t-test. (e) Haematopoietic activity in D4 EBs in ES cells that had been engineered to inducibly express Smad1 carrying a mutation at the GSK3 β conserved site (S210) or WT Smad1. Dox was added from day 2 to 4 of EB differentiation and CHIR99021 was added from day 3 to 4. Bars indicate s.e.'s from three independent experiments. * $P < 0.05$, ** $P < 0.01$, *** $P < 0.001$ by t-test. (f) Integrative Genome Viewer (IGV) tracks for *Id1*, *Id2* and *Id3* genomic regions from Smad1 ChIP-seq experiment performed on D4 EBs treated for 24 h with dimethylsulphoxide (DMSO) or IWR-1. Squares indicate Smad1 bound regions. Scale bar, 2 Kb. (g) Validation of Smad1 binding at the *Id1* (-1 Kb) and *Id2* (-2 Kb) sites by ChIP-qPCR. Graph represents the average plus s.e. from five independent experiments. IWR-1 treatment decreases Smad1 binding at these two sites. * $P < 0.05$ by t-test. (h) Tag density distribution of ChIP-seq reads across a \pm 3 kb region centered on Smad1 peaks. IWR-1 treatment affects the genome wide binding of Smad1.

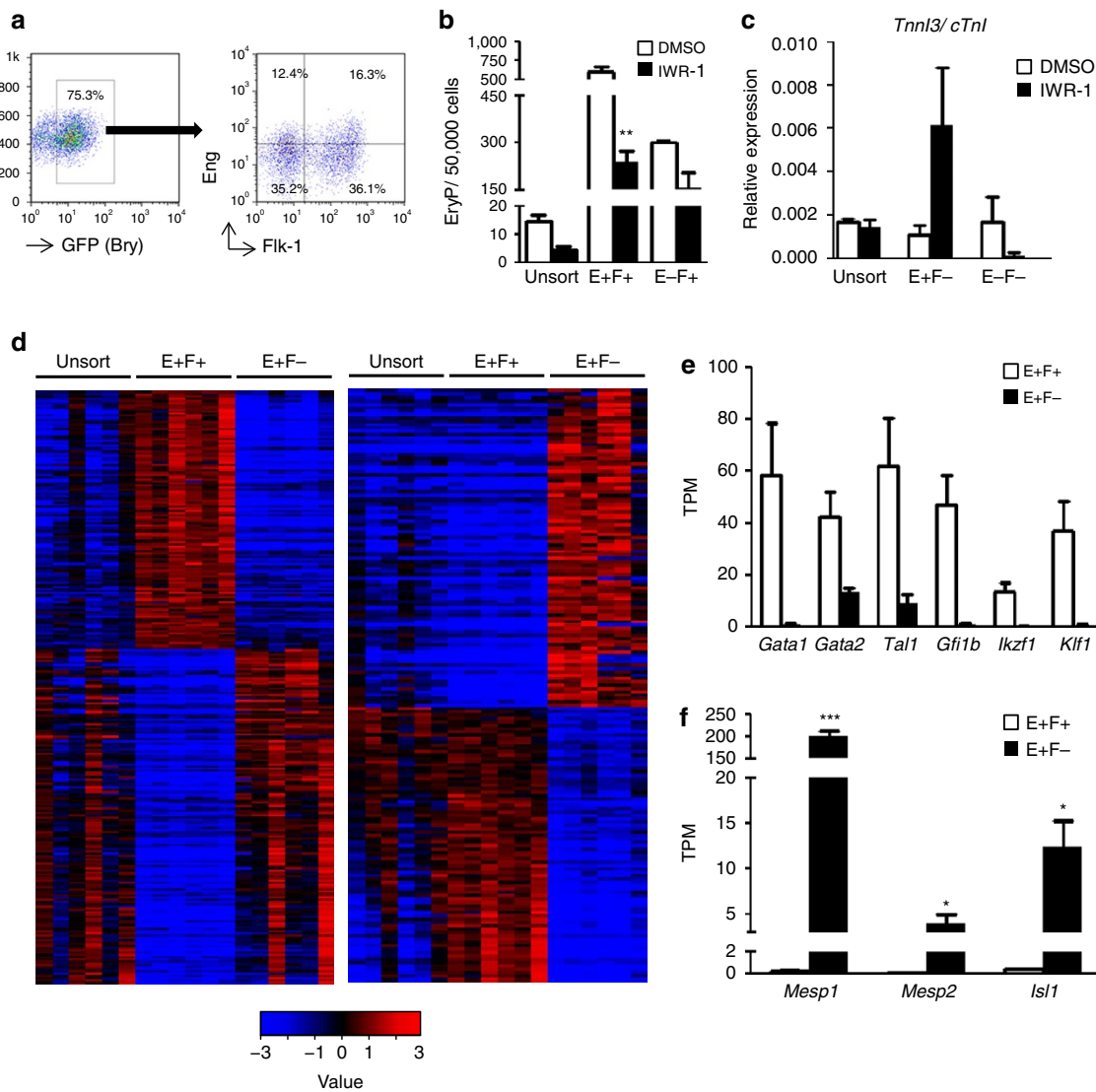


Figure 3 | Endoglin identifies cells with both hematopoietic and cardiac potential from Bry⁺ mesoderm. (a) Representative FACS plots show GFP (Bry) expression in day 3 EBs (left) and subsequent analysis of gated GFP⁺ (Bry⁺) cells for the expression of Eng and Flk-1 (right). Subfractions were sorted, reaggregated for 24 h and subsequently used for analysis (b,d-f) or further differentiation (c). (b) Primitive erythroid colony activity in E⁺F⁺ and E⁺F⁻, and unsorted reaggregates show increased numbers of EryP colonies in the E⁺F⁺ subfraction (white bar), which is specifically abrogated by IWR-1 (black bar). Bars indicate s.e.'s from three independent experiments. **P<0.01 by t-test. (c) Cardiac potential. Reaggregates from unsorted, E⁺F⁻ and E⁺F⁻ subfractions were plated as monolayer for 5 days in the presence of IWR-1 or dimethylsulphoxide (DMSO) and analysed for the expression of *Tnni3/cTnI*. (d-f) Heatmap of RNA-Seq analysis shows genes that are distinctly expressed in either E⁺F⁺ or E⁺F⁻ (d). Analyses were performed with three independent biological samples. Values are log₂(estimated expression/mean estimated expression of the row), with blue indicating negative values. (e) Expression levels of selected hematopoietic genes found upregulated in the E⁺F⁺ subfraction are shown as median-normalized transcripts per million (TPM). (f) Early cardiac transcription factors *Mesp1*, *Mesp2* and *Isl1* are selectively expressed in the E⁺F⁻ subfraction. *P<0.05; ***P<0.001 by t-test.

only in the E⁺F⁻ group with IWR-1 (Supplementary Movies 1–3). These observations were corroborated by analyses for the cardiac functional *Tnni3* gene (Fig. 3c), which showed prominent expression in the Bry⁺E⁺F⁻ (fourfold higher than unsorted and Bry⁺E⁺F⁻). These results reveal that Eng identifies hematopoietic and cardiac progenitors within early Bry⁺ mesoderm.

To further characterize the molecular signature of these early Bry⁺E⁺F⁺ and Bry⁺E⁺F⁻ blood and cardiac subpopulations, we performed transcriptional profiling by RNA-Seq (Fig. 3d). Among the genes exclusively upregulated in the E⁺F⁺ population, we found *Gata1*, *Gata2*, *Tal1/Scl* and *Klf1* (Fig. 3e), which are known to regulate primitive erythropoiesis during

embryogenesis^{26–28}, as well as *Gfi1b* (Fig. 3e). On the other hand, the E⁺F⁻ population was characterized by high expression of *Mesp1*, *Mesp2* and *Isl1* (Fig. 3f), key regulators of early cardiac specification^{29,30}. *Gata4* expression was also found significantly upregulated in the E⁺F⁻ population, while other cardiac-specific genes, *Nkx2.5*, *Tbx5*, *Mef2C* and *Hand2* were expressed at very low levels at this early developmental stage (Supplementary Fig. 3b). These findings are in agreement with the data obtained in the hematopoietic and cardiac assays (Fig. 3b,c; Supplementary Movies 1–3), and confirm that E⁺F⁺ and E⁺F⁻ are, respectively, endowed with hematopoietic and cardiac potential, demonstrating that Eng marks not only hematopoietic potential but also cardiac cell fate within the mesoderm population.

Jdp2 mediates Eng's effects on haematopoiesis. To define how Eng-mediated BMP and Wnt modulation promotes haematopoietic commitment, we identified genes differentially expressed by IWR-1 in the E⁺F⁺ population (Fig. 4a). Among the genes showing differential expression in the control compared to IWR-1 group, we prioritized *Jdp2* and *Epas1* as candidates. These genes have been reported to be important for adult haematopoiesis^{31,32}, and our data suggest a novel function in early cell fate

specification. The expression levels of these genes were validated by qPCR, and the expression of *Jdp2* and *Epas1* was distinctively inhibited by IWR-1 in the E⁺F⁺ population (Fig. 4b,c).

Recently, Han and colleagues have documented high-resolution RNA sequencing analysis on single mid-gastrulation mouse embryos to assemble a spatial transcriptome that correlated with the patterning of cell fates within the embryo³³. Using the web portal iTriTranscriptome (www.itranscriptome.org)³³, we analysed

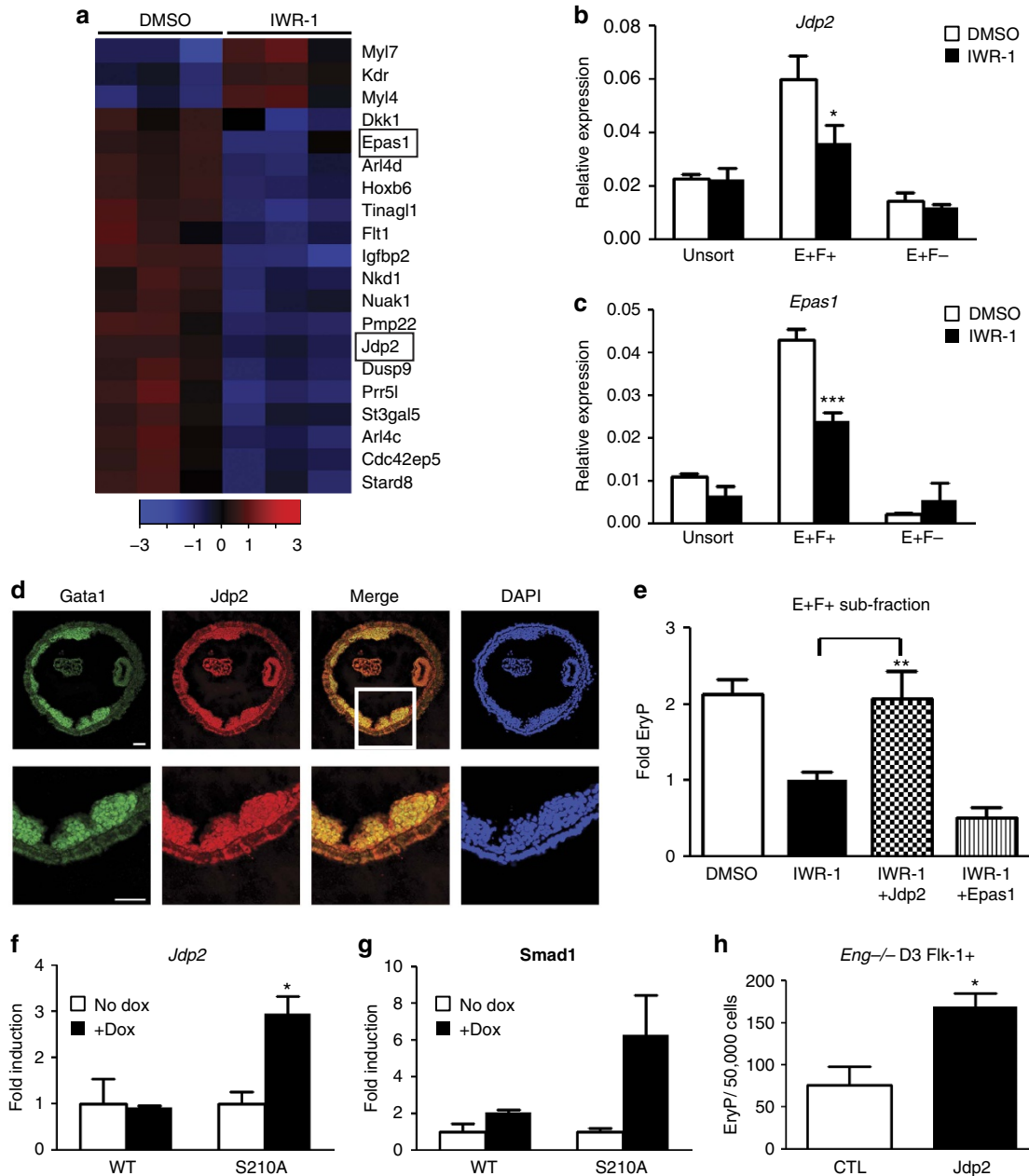


Figure 4 | Jdp2 is a target of Eng-mediated BMP and Wnt signals to enhance haematopoietic commitment. (a) Heatmap of E⁺F⁺ RNA-seq from EB samples treated either with dimethylsulphoxide (DMSO) or IWR-1. Heatmap values are log₂(estimated expression/mean estimated expression of the row), with blue indicating negative values. (b,c) Validation qPCR confirms that haematopoietic candidate genes *Jdp2* (b) and *Epas1* (c) are mostly expressed in the E⁺F⁺ fraction, and this is counteracted by IWR-1. Data represent three independent biological samples. *P<0.05; ***P<0.001 by t-test. (d) Confocal images of E7.5 YS cryosections reveal that *Jdp2* is expressed in *Gata1*⁺ primitive erythrocytes present within the blood island. Close-up images (white box) are shown in the lower panel. 4,6-Diamidino-2-phenylindole (DAPI) stains the nuclei. Scale bars, 50 μ m. (e) Enforced expression of *Jdp2* rescues erythroid colony activity in E⁺F⁺ cells cultured in the presence of IWR-1, whereas *Epas1* does not. Bars indicate s.e.'s from three independent experiments. **P<0.01 by one-way analysis of variance. (f,g) Expression levels of *Jdp2* (f) and *Smad1* (g) in day 4 EBs from inducible WT and S210A mutant *Smad1* ES cells. Transcript levels are normalized to no dox group. Bar indicates s.e.'s from two independent experiments. *P<0.05 by t-test. (h) Enforced expression of *Jdp2* rescues impaired primitive erythroid colony activity of Flk-1⁺ cells from *Eng*^{-/-} day 3 EBs. Bars indicate s.e.'s from two independent experiments. *P<0.05 by t-test.

the expression pattern of various genes expressed in the E⁺F⁺ population (Supplementary Fig. 3c). In support of our RNA-Seq data, we found the expression pattern of *Jdp2* and *Epas1* to be co-localized to that of *Eng* as well as the haematopoietic transcription factor *Gata2*, which were observed in the posterior region at this developmental stage. Interestingly, this region was also found to co-express *Bmp2* and *Wnt3*.

Since the earliest haematopoietic precursors express *Eng* during embryogenesis⁹, we examined *Jdp2* expression in E7.5 embryos. Confocal imaging showed expression of *Jdp2* at this early developmental stage, with the majority of *Jdp2*⁺ cells co-expressing GATA1, indicative of primitive erythrocytes (Fig. 4d). Considering that a subpopulation of *Eng*⁺ cells co-expresses *Gata1* in E7.5 YSs⁹, these data further corroborate *Jdp2* as a target of *Eng* and a novel regulator of early haematopoiesis.

Next, we determined whether *Jdp2* or *Epas1* would have the capacity to rescue the impaired haematopoiesis observed when E⁺F⁺ cells are exposed to IWR-1 (Fig. 3b). For these rescue experiments, E⁺F⁺ cells were transduced with lentiviral constructs encoding *Jdp2* or *Epas1* and control vector, reaggregated in the presence of IWR-1 for 24 h, and plated for scoring haematopoietic colony activity. Whereas transduction with *Epas1* did not rescue blood formation, *Jdp2* was able to counteract the inhibitory effects of IWR-1 on the haematopoietic colony activity of E⁺F⁺ cells (Fig. 4e).

Importantly, iSmad1 S210A mutant day 4 EB cultures that exhibit enhanced haematopoietic colony activity (Fig. 2e), express significantly higher levels of *Jdp2* (Fig. 4f), which correlated with *Smad1* expression (Fig. 4g). To further evaluate the effect of *Jdp2* in haematopoiesis, we used a haematopoietic reporter transgenic zebrafish, in which DsRed labels haematopoietic cells that are positive for *gata1*³⁴. For this, *Tg(gata1:DsRed)* zebrafish embryos at the 1–2-cell stage were injected with *jdp2*-GFP mRNA or with control *venus* mRNA. In accordance with the findings described above (Fig. 4d–f), *jdp2*-injected embryos displayed enhanced haematopoiesis, as demonstrated by the increased levels of DsRed (*gata1*⁺) when compared with *venus*-injected control embryos at 48 h.p.f. (Supplementary Fig. 3d). Since the lack of *Eng* during early blood development results in impaired haematopoietic activity^{9,10}, which is accompanied by decreased Smad1 phosphorylation^{8,35}, we next examined whether enforced *Jdp2* expression would counteract the defective haematopoietic phenotype of *Eng*-null EBs. Flk-1⁺ cells isolated from day 3 *Eng*^{−/−} EBs were transduced with *Jdp2*-encoded lentiviral vector or empty vector (control), reaggregated for 24 h, and assayed for haematopoietic colony activity. Significantly increased numbers of haematopoietic colonies were observed upon *Jdp2* induction (Fig. 4g), revealing that *Jdp2* is an important downstream effector of *Eng*. This finding was subsequently validated *in vivo* using *Eng*-deficient E9.5 YSs, which have defective haematopoietic development⁹. *Jdp2*-encoding and GFP control lentiviral vectors were introduced into *Eng*-null (KO) and littermate control (CTL) YSs, and haematopoietic activity was enumerated following their direct plating into methylcellulose-based medium containing haematopoietic cytokines. In agreement with the *in vitro* EB data, we observed rescued haematopoiesis upon *Jdp2* transduction in *Eng*-null YS (Supplementary Fig. 3e). Together, these data demonstrate that *Jdp2* is a key target coordinately regulated by Wnt and *Eng* that is sufficient to establish haematopoietic fate in early mesoderm.

Discussion

Our study has revealed *Eng* as a critical modulator of the crosstalk observed between BMP and Wnt signalling pathways

during early cell fate specification of the cardiac and haematopoietic lineages. In this context, *Eng* ensures the commitment of *Bry*⁺ mesodermal precursors (GFP⁺*Eng*⁺) towards the haematopoietic lineage by repressing the cardiac program in hemogenic sites. Importantly, we have identified *Jdp2* as a target of *Eng*-mediated BMP and Wnt signalling, providing a molecular mechanism that illustrates how signalling pathways and their targets orchestrate the haematopoietic commitment of mesoderm.

During embryogenesis, BMP signals are not only required for mesoderm induction but also for blood commitment³⁶. Moreover, forced expression of *Smad1* enhances hemangioblast activity and the haematopoietic commitment of these cells towards the haematopoietic lineage³⁷. Similar to BMP, the Wnt signalling pathway plays pivotal roles in development³⁸, and specifically in the haematopoietic system, Wnt signals are required for primitive haematopoiesis^{39,40}. Interestingly, crosstalk between BMP and Wnt has been reported to be involved in the activation of the haematopoietic program in mesodermal cells^{5,6}. Our findings provide key insights into the mechanism behind this crosstalk, as they reveal that *Eng* modulates BMP and Wnt signals to enhance *Smad1* activity and ultimately haematopoiesis. We further demonstrated that BMP and Wnt integration via *Smad1* is critical to regulate gene expression in mesodermal cells. Notably, *Smad1* binding was detected at *Tbx5*, suggesting a potential mechanism of *Smad1*-mediated *Tbx5* repression. Accordingly, reduced levels of *Tbx5* have been reported upon *Eng* induction⁷. Moreover, we revealed that *Jdp2* is regulated by *Eng*-mediated BMP and Wnt modulation and plays a critical function in promoting the haematopoietic commitment from early mesoderm. *Jdp2*, an AP-1 family transcription factor, has been reported to modulate chromatin by inhibiting histone acetyltransferase activity⁴¹. Interestingly, *Jdp2* expression was shown to be important for the lymphoid versus myeloid lineage decision by modulating DNA methylation⁴². Neutrophil activity has been reported to be impaired in *Jdp2*^{−/−} mice⁴³. A function for *Jdp2* during embryogenesis had not previously been documented. Based on these studies, we speculate that BMP- and Wnt-mediated *Jdp2* induction may be required for directing epigenetic modification of mesodermal progenitors, allowing them to acquire the haematopoietic fate.

Together, our data support the notion that *Eng* is critical for the crosstalk between BMP and Wnt pathways during development and contribute to broaden our understanding of the transforming growth factor- β superfamily signalling in embryonic cell fate decisions.

Methods

Generation of inducible ES cell lines. WT mSmad1 (ref. 44) was subcloned into the p2Lox TEV FLAG targeting vector. p2Lox TEV FLAG vector was generated by inserting the sequence 5'-CTGCAGGCTAGCggggcGAGATAAAAGACGATGACCAAGTAG-3' flanked by EcoRI and NotI sites into the p2lox plasmid. Smad1 S210A mutant was generated using the Quickchange Mutagenesis kit (Stratagene) following the manufacturer's instructions. Smad1 WT and Smad1 S210A inducible ES cells were generated in A2Lox ES cells⁷. To generate 7TFC:Eng ES cells, iEng ES cells were transduced with a lentiviral vector expressing 7Tcf-FFluc/SV40-mCherry (7TFC, Addgene). iEng ES cells containing the 7TFC transgene were obtained following two rounds of FACS sorting based on mCherry expression using a FACS ARIA instrument (BD).

Growth and differentiation of ES cells. In addition to the generated ES cell lines described above, E14, *Bry*/GFP-reporter²⁵, *Eng*^{−/−}¹⁰ and iEng ES cells⁷ were used in this study. ES cell lines were cultured on irradiated mouse embryonic fibroblasts in DMEM (Gibco) supplemented with 1,000 U ml^{−1} LIF (Millipore), 15% inactivated fetal bovine serum (Gibco), 0.1 mM non-essential amino acids (Gibco) and 0.1 mM of β -mercaptoethanol (Sigma). For EB differentiation, ES cells were preplated for 30 min to remove mouse embryonic fibroblasts and then plated in hanging drops (100 cells per 10 μ l drop) in EB differentiation medium, IMDM

(Gibco) supplemented with 15% fetal bovine serum (FBS; Gibco), 4.5 mM monothioglycerol (Sigma), 100 μ g ml $^{-1}$ ascorbic acid (Sigma) and 200 μ g ml $^{-1}$ iron-saturated transferrin (Sigma) in 150 mm Petri dishes. After 48 h, EBs were collected and resuspended into 10 cm Petri dishes in 10 ml of EB differentiation medium. These dishes were cultured on a slowly swirling table rotator (80 r.p.m.). To induce appropriate Eng expression during EB differentiation, doxycycline (Sigma) was added to the cultures, at 1 μ g ml $^{-1}$, beginning at day 2, except for time window studies. In the studies involving iSmad1 ES cell lines, 3 μ M of CHIR99021 or dimethylsulphoxide (vehicle) was added to EB cultures at day 3.5 and 24 h later, cells were collected for EryP CFC assay.

Zebrafish embryology and imaging. WT and transgenic zebrafish lines, *Tg(7xTCF:mCherry)*¹⁹, *Tg(cmhc2:EGFP)*⁴⁵ and *Tg(gata1:DsRed)*³⁴ were maintained according to the IACUC, UMN approved protocols. The full length of Eng CDS (WT) was PCR amplified using human ENDOGLIN cDNA (Dharmacon, MHS1010-202743199). ENDOGLIN deletion mutant (Δ OD)²⁰ was generated using the Quickchange Mutagenesis kit (Stratagene) following the manufacturer's instructions. Then, amplified DNA was cloned into pCS2+ vector. The zebrafish *jdp2*-GFP construct was generated by synthesis of a double-stranded DNA fragment (gBlock, IDT), containing zebrafish *jdp2* CDS without stop codon and flanked by Nhe1 sites. This fragment was subsequently cloned into pCS2-T2A-GFP vector and sequenced. mRNA was synthesized using the mMESSAGE mACHINE SP6 kit (Ambion) according to the manufacturer's instructions. Zebrafish embryos were injected with 100 pg of control (*venus* or *mCherry*) or human *ENG* mRNAs (WT and Δ OD) at the one–two-cell stage. For confocal live imaging, micro-injected *Tg(cmhc2:EGFP)* embryos were mounted in low-melt agarose, and imaged using an LSM710 confocal microscope (Carl Zeiss Microscopy). For *in vivo* Wnt signalling tracing, micro-injected *Tg(7xTCF:mCherry)* embryos were dissociated in 0.25% trypsin for 3 min at 37 °C and analysed based on mCherry fluorescence by flow cytometry. For counting cardiac progenitors, micro-injected *Tg(cmhc2:EGFP)* embryos were dissociated in 0.25% trypsin for 3 min at 37 °C and analysed based on EGFP fluorescence by flow cytometry. For evaluation of haematopoiesis, 50 ng of control (*venus*) or zebrafish *jdp2*-GFP mRNAs were injected into *Tg(gata1:DsRed)* embryos. mRNA-injected embryos were dissociated in 0.25% trypsin for 5 min at 37 °C and analysed by flow cytometry for DsRed fluorescence at 48 h.p.f. Approximately 20 embryos were grouped as one sample for qPCR with reverse transcription and cell sorting experiments.

Mice and embryo explants. All animals were handled in strict accordance with good animal practice as defined by the relevant national and/or local animal welfare bodies, and all animal work was approved by the University of Minnesota Institutional Animal Care and Use Committee. Male heterozygous mice bearing an EGFP knock-in into the *Brachyury* locus (GFP/*Bry*^{+/−})⁴⁶ were mated with CD-1 IGS female mice (Charles River Laboratories). *Eng*-deficient embryos were generated by timed mating *Eng*^{+/−} heterozygotes, or *Eng*^{Δ/Δ} to *Eng*^{wt/Δ}, as previously described^{9,47}. Dox-iEng embryos were generated by timed mating of iEng mice. All YSs were dissociated in 0.25% trypsin for 3 min at 37 °C.

Generation of iEng transgenic mice. The Dox-iEng ES cell line was generated as previously reported⁷. Mice were derived from the iEng ES cells through blastocyst injection, crossed C57/BL6 to establish a founder bearing the iEng gene and then bred to Rosa-rtTA2SM2 mice⁴⁸ to establish an iEng mouse. Transgenic mice were screened for DNA integration by PCR. To induce Eng expression during gastrulation, 100 μ l of 10 mg ml $^{-1}$ doxycycline (Sigma) was given IP to E7.5 time pregnant iEng females.

Flow cytometry and FACS sorting. Trypsinized EB cells were resuspended in PBS supplemented with 10% FBS containing 0.25 μ g per 10 6 cells of Fc block (eBioscience) and incubated on ice for 5 min. PE-Cy7-conjugated (BioLegend) or PE-conjugated (eBioscience) anti-mouse Eng/CD105 and APC-conjugated anti-mouse Flk-1 (eBioscience) antibodies were added at 0.5 μ g per 10 6 cells and incubated at 4 °C for 20 min before washing with PBS. We analysed stained cells on a FACS Aria after adding propidium iodide (Pharmingen) to exclude dead cells. Day 3 EBs from *Bry*/GFP ES cells were gated based on GFP expression, and then purified based on the expression of Eng and Flk-1. Individual E8.5 iEng embryo was removed from YS and dissected into head forming region. Both YSs and head forming region of embryos were dissociated in 0.25% trypsin for 3 min at 37 °C. Trypsinized embryos and YSs were analysed by flow cytometry using PE-conjugated anti-mouse PDGFR α , APC-conjugated anti-mouse Flk-1 (eBioscience) and PE-Cy7-conjugated anti-mouse Eng/CD105 (BioLegend) antibodies. Trypsinized zebrafish embryos were stained with PE-conjugated anti-human Eng/CD105 antibody (eBioscience). All antibodies were added at 0.5 μ g per 10 6 cells. Data were analysed using FlowJo Version 7.6.5 software (TreeStar).

Lentiviral transduction. Cells that had been dissociated from E8.5 GFP/*Bry*^{+/−} embryo explants were transduced either with empty vector control (pSAM-iresGFP) or a lentiviral vector encoding Eng (pSAM-Eng), reaggregated in 1 ml EB

medium on low-adherent 24-well plates. After 24–48 h, reaggregates were used for cardiac differentiation studies, as described below. For differentiating ES cells, the E $^+$ F $^+$ subfraction purified from day 3 *Bry*/GFP EBs were transduced either with lentiviral vector encoding *Jdp2* (pRRL-*Jdp2*) or *Epas1* (pRRL-*Epas1*). As a control, a cohort was transduced with empty vector (pRRL-dsRed). For E9.5 YSs, dissociated YSs were divided in two and transduced either with lentiviral vector encoding *Jdp2* (pRRL-*Jdp2*) or empty vector (pRRL-GFP). Spin-infections were performed at 1,100g for 1 h and 30 min at 30 °C and then incubated in the presence of the lentivirus for an additional 24 h at 37 °C.

Haematopoietic CFC assays. Cells from day 4 EBs or reaggregates were plated at 5 \times 10 4 cells into 1.5 ml of methylcellulose medium containing interleukin-3, interleukin-6, erythropoietin (EPO) and SCF (M3434; StemCell Technologies). In the studies involving YS, 10,000 cells from E8.5 iEng YSs or E9.5 Eng-floxed YSs were plated directly into M3434 and cultured in a humidified low-oxygen (5%) incubator at 37 °C. Primitive erythroid colonies were counted after 5 days, and definitive haematopoietic colonies were scored 7–10 days after plating.

Cardiac differentiation. Reaggregates from EB-sorted cells were plated on gelatinized plates in IMDM medium with 2% FBS and 10 μ M IWR-1 (Sigma). Reaggregates from E8.5 embryo explants were plated on OP9 monolayer in the absence or presence of 10 μ M IWR-1.

Immunofluorescence staining. Cells for immunofluorescence staining were fixed with 4% paraformaldehyde in PBS, and blocked with 5% bovine serum albumin (BSA) in PBS. cTnI (1:250, Abcam) and anti-Goat Cy3 (1:500, Jackson Laboratory) were used as primary and secondary antibodies, respectively. To detect the nuclei, after washing, samples were stained with HOECHST H1399 (1:2,000, Life Technologies). For quantification, the size of cTnI-positive (cTnI $^+$) cells from embryo explants were measured by ImageJ (NIH). For YS analysis, dissected embryos were fixed in 2% paraformaldehyde for 20 min, subsequently incubated in 5 and 15% sucrose solutions until embryos decanted and then frozen in 7.5% gelatin. Cryosections were incubated with anti-*Jdp2* (1:100, Santa Cruz) and anti-*Gata1* (1:100, Santa Cruz) antibodies overnight at 4 °C. Reactions were detected after 1 h of incubation with anti-Rabbit Alexa Fluor 555 (1:400, Invitrogen) and anti-Rat 488 (1:400, Jackson Laboratory). Staining was visualized by laser confocal scanning (Zeiss LM510).

Western blotting. EB cell lysates were prepared using 1 \times RIPA buffer (150 mM NaCl, 50 mM Tris-HCl, pH 7.5, 1 mM EDTA, 1% Triton, 1% sodium deoxycholate and 0.1% SDS) supplemented with Complete Protease Inhibitor Cocktail (Roche) and PhosSTOP (Roche), and quantified with Bradford reagent (Sigma). Samples were prepared in Laemmli buffer (BioRad) and loaded on gels for SDS-polyacrylamide gel electrophoresis. Proteins were transferred to a polyvinyl difluoride membrane (Millipore). The following primary antibodies were applied at the indicated dilution in Primary Antibody Signal Boost Immunoreaction Enhancer (Calbiochem); phosphorylated Smad1/5/8 (S465/8 and S426/8, 1:1,000, Cell Signaling), Smad1 (1:3,000, Abcam), cTnI (1:1,000, Abcam), β -actin Catenin (1:1,000, Millipore), pGsk3 α / β (S21/S9, 1:1,000, Cell Signaling). Gapdh (Abcam) and actin (Millipore) were diluted at 1:3,000 with 5% BSA in 1 \times TBS-Tween 20. All primary antibodies were incubated for 12 h at 4 °C on a shaker. Enhanced chemiluminescence peroxidase-labelled anti-mouse and anti-rabbit antibodies (GE Biosciences) were diluted at 1:20,000 with 5% BSA in 1 \times TBS-Tween 20. After washing the membranes, SuperSignal West Pico Chemiluminescent Substrate (ThermoScientific) was utilized to detect the horseradish peroxidase signal. All uncropped western blots can be found in Supplementary Fig. 4.

Reporter assay. Wnt activity was measured in iEng;7TFC reporter ES cells, in which fire fly luciferase reflects β -catenin expression (7xTcf-FFluc/SV40-mCherry; Addgene). To stimulate the Wnt pathway, 3 μ M CHIR99021 (Millipore) was added to the culture medium at day 3 of EB differentiation. EBs were collected at 30 min, 1 and 3 h after Wnt stimulation. A control sample was collected before Wnt stimulation, which we consider 0 h sample. To measure bioluminescence in these samples, we utilized the Dual-luciferase reporter assay system (Promega), and luciferase activity was analysed using the Sirius Luminometer (Berthold Detection Systems).

RNA isolation, gene expression and RNA-Seq. Cells from explants, YSs, zebrafish embryos and total EBs were resuspended in Trizol (Life Technologies) and processed following the manufacturer's instructions. RNAs from sorted cells were retro-transcribed using Superscript Vilo (Life Technologies) and the rest RNAs were retro-transcribed using Thermoscript (Life Technologies). TaqMan probes (Life Technologies) were used. For globins, we designed customized primer/probe sets (all shown 5'-3'): beta-major F, AGGGCACCTTG CCAGC; beta-major R, GGCAGCCTCTGCAGCG; beta-major probe, 6FAM-CGTGATTG TGCTGGGCCACCACCT-TAMRA. Embryonic F, CCTCAAGGAGACCT

TTGCTCAT; embryonic R, CAGGCAGCCTGCACCTCT; embryonic probe, 6FAM-CAACATGTTGG TGATTGTCCTTCT-TAMRA.

For RNA-Seq, 100 ng of total RNA for each sample was treated with DNase1 amplification grade (Life Technologies) following the manufacturer's instructions. Sequencing libraries were generated from 100 ng of total RNA using the TruSeq RNA Sample Preparation kit (Illumina) and quantitated using the Qubit fluorometer (Life Technologies) following the manufacturer's instructions. The libraries were then pooled six samples per lane using 35 ng per sample for a 51 + 8 + 8 cycle (to accommodate 8 + 8 indexed samples in other lanes) Single Read run on the HiSeq 2500 (Illumina) by high-output run sequencing. The sequencer outputs were processed using Illumina's CASAVA-1.8.2 basecalling software. Demultiplexing assigned ~475 million reads across the 18 samples, ranging from 23 to 30 million reads per sample. Of the assigned reads, ~2.5 million were discarded for low quality or the presence of sequencing adaptors in the reads. Each sample's reads were then processed using RSEM version 1.2.3 (with bowtie-0.12.9 for the alignment step)^{49,50}. Percentage of reads mapped to the transcriptome ranged from 88 to 93%.

ChIP, library generation, sequencing and data analysis. ChIP was performed following the protocol described by Young and colleagues⁵¹ with minor modifications. In brief, D4 EBs were trypsin-treated at 37 °C for 1 min with gentle shaking and reaction was inhibited by adding 10%FBS/PBS. Single cells were washed once with PBS, resuspended in 10%FBS/PBS and supplemented with formaldehyde (final concentration 1%) for crosslinking of protein-DNA complexes (10 min at room temperature) followed by quenching with glycine. Cells were snap-frozen in liquid nitrogen and stored at -80 °C if not processed immediately. Cell pellets were incubated in lysis buffer LB1 supplemented with protease inhibitors (50 mM HEPES KOH, pH7.5, 140 mM NaCl, 1 mM EDTA, 10% glycerol, 0.5% NP40, 0.25% Triton X-100 + Complete-mini—Roche) for 10 min at +4 °C followed by incubation in buffer LB2 supplemented with protease inhibitors (10 mM Tris-HCl, pH 8, 200 mM NaCl, 1 mM EDTA, 0.5 mM EGTA + Complete-mini—Roche) for 10 min at +4 °C. Cell pellet was then resuspended in LB3 supplemented with protease inhibitors (10 mM Tris-HCl, pH 8, 100 mM NaCl, 1 mM EDTA, 0.5 mM EGTA, 0.1% sodium deoxycholate, 0.5% N-lauroylsarcosine + Complete-mini—Roche) and then sonicated with a Bransonic sonicator at 18% power for 1 min with intervals of 10 s ON-10 s OFF. Each sample was subjected to five to six cycles of sonication to reach an average chromatin size of 300 bp. After shearing, samples were centrifuged for 10 min at 16,000g and snap-frozen in liquid nitrogen if not processed immediately. For each ChIP, 20 µg of chromatin (diluted to 400 µl) was precleared for 4 h at 4 °C with 15 µl of BSA-blocked Protein A-conjugated sepharose beads (GE healthcare) and then supplemented with 1/10 volume of 10% Triton X-100. Immunoprecipitation was performed by overnight incubation with normal rabbit IgG (8 µg—Santa Cruz Biotechnology) or anti-Smad1 antibody (1:25—Cell Signaling Technology #9743). Immune complexes were recovered by incubation with 15 µl of BSA-blocked Protein A-conjugated sepharose beads for 4 h at 4 °C and then washed five times with RIPA wash buffer (50 mM HEPES KOH, pH7.5, 500 mM LiCl, 1 mM EDTA, 1% NP40, 0.25% Triton X-100 and 0.7% sodium deoxycholate) and one time with TEN buffer (10 mM Tris-HCl, pH 8, 1 mM EDTA and 50 mM NaCl). Immunoprecipitated chromatin was recovered by incubating beads with 200 µl of elution buffer (50 mM Tris-HCl, pH 8, 10 mM EDTA and 1% SDS) for 20 min at 65 °C. Chromatin from immunoprecipitation and input (equivalent to 1% of starting material) was reverse crosslinked overnight at 65 °C, then diluted 1:1 with TE (10 mM Tris-HCl, pH 8, and 1 mM EDTA) supplemented with 4 µl of RNaseA 20 mg ml⁻¹ and incubated for 2 h at 37 °C followed by Proteinase K treatment (4 µl of 20 mg ml⁻¹ stock for each sample) for 30 min at 55 °C. DNA was purified by Phenol-chloroform-isoamyl alcohol extraction (twice) followed by chloroform extraction, then supplemented with 1/10 of volume of 3 M sodium acetate, pH 5, and 1.5 µl of glycogen and precipitated with two volumes of 100% ethanol at -80 °C for >1 h. Followed 30 min centrifuge at 16,000g, pellet was washed with 75% ethanol, air-dried and dissolved in 45 µl H₂O. qPCR was performed in a final volume of 10 µl using SYBR Premix Ex Taq II (Clontech), 0.5 µl of 1.4 µM primer stock and 0.3 µl sample/reaction, and run on a 384-well plate on a ABI7900HT instrument (Applied Biosystems). The following primers were used for qPCR. Id1 - 1 Kb-FW: 5'-AGCCGTCCGGGTTTATG-3'; Id1 - 1 Kb-RV: 5'-GTGTCAG CGTCTGAACAAGC-3'; Id2 - 2 Kb-FW: 5'-CCCTGACGCCTTGCTTC-3'; Id2 - 2 Kb-RV: 5'-CCTTCAGGGATTGATCAGC-3'; Tbx5 + 6 Kb-FW: 5'-TGGA TCTCACGGAGGATGGA-3'; Tbx5 + 6 Kb-RV: 5'-GGGCGAGATTCTGTGCA GATA-3'.

Libraries were generated following a gel-free protocol using AMPure XP beads (Beckman Coulter) for all the purification and size selection steps. An amount of 10 ng or less of DNA was end-repaired using End-it DNA end repair (Epicentre), then A-tailed using Klenow Fragment (3'→5' exo⁻, NEB) followed by adapter-barcode ligation using T4 DNA ligase (Enzymatics). Illumina compatible adapter-barcodes were purchased from BIOO scientific. After ligation, DNAs were negatively size selected using 0.5× Ampure XP beads and unbound DNAs were positively size selected using 0.4× Ampure XP beads (this step allows for retention of DNA fragments ranging 200–500 bp). Libraries were amplified using Phusion High Fidelity PCR master mix 2× (NEB) with a 16-cycle program. Purified libraries were then submitted to the University of Minnesota Genomic

Center (UMGC) for quantification, quality control and sequencing. Libraries were pooled and sequenced on a lane of Single-End run on a HiSeq2500 operated at High-Output mode (Illumina). The sequencer outputs were processed using the Galaxy platform⁵² available at the Minnesota Supercomputing Institute. Demultiplexing assigned ~134 million reads across the four samples, ranging from 30 to 36 million reads per sample. Each sample's reads were then aligned to the mouse genome (mm10) using Bowtie2 (ref. 53) followed by the removal of PCR duplicates using the SAM tool rmdup 1.0.1 (ref. 54). Peak calling was performed using both MACS 1.0.1 (ref. 55) (parameters: -s 51 -bw 300, -p 1e-05 -m 32) and QESEQ⁵⁶ (parameters: -s 100 -c 15 -p 0.05) and only common peaks between the outputs of both algorithms were further considered. Biwig files for visualization on IGV⁵⁷ were generated by converting the wig files obtained from MACS using the Galaxy tool Wig-to-BigWig. Density maps were generated with SeqMiner⁵⁸ using the enrichment file enr.sgr produced by QESEQ.

Statistical analysis. Differences between two groups were assessed by using the Student's *t*-test. Differences between multiple groups were assessed by analysis of variance. The R package EBSeq⁵⁹ was used to identify genes expressed differentially between one sample type and one or more others. Those genes reported by EBSeq to have a posterior probability of differential expression of 0.50 or greater were then filtered to select only those with median-normalized TPM > 16 in at least one sample, and a fold change of at least 2 between the mean of the median-normalized expected counts (EC) of the control samples versus that of the others. Heatmaps of relative expression display for each gene G and sample S the value log₂((1 + median-normalized EC(G,S))/(1 + mean overall S_i median-normalized EC(G, S_i)).

Data availability. RNA-Seq data that support the findings of this study have been deposited in the Gene Expression Omnibus (GEO) database under accession code GSE85855. ChIP-seq data have been deposited in the GEO database under accession code GSE85797. All other relevant data are available from the corresponding author on request.

References

- Marvin, M. J., Di Rocco, G., Gardiner, A., Bush, S. M. & Lassar, A. B. Inhibition of Wnt activity induces heart formation from posterior mesoderm. *Genes Dev.* **15**, 316–327 (2001).
- Schoenebeck, J. J., Keegan, B. R. & Yelon, D. Vessel and blood specification override cardiac potential in anterior mesoderm. *Dev. Cell* **13**, 254–267 (2007).
- Arnold, S. J. & Robertson, E. J. Making a commitment: cell lineage allocation and axis patterning in the early mouse embryo. *Nat. Rev. Mol. Cell Biol.* **10**, 91–103 (2009).
- Song, J. *et al.* Smad1 transcription factor integrates BMP2 and Wnt3a signals in migrating cardiac progenitor cells. *Proc. Natl Acad. Sci. USA* **111**, 7337–7342 (2014).
- Lengerke, C. *et al.* BMP and Wnt specify hematopoietic fate by activation of the Cdx-Hox pathway. *Cell Stem Cell* **2**, 72–82 (2008).
- Nostro, M. C., Cheng, X., Keller, G. M. & Gadue, P. Wnt, activin, and BMP signaling regulate distinct stages in the developmental pathway from embryonic stem cells to blood. *Cell Stem Cell* **2**, 60–71 (2008).
- Baik, J., Borges, L., Magli, A., Thatava, T. & Perlingeiro, R. C. Effect of endoglin overexpression during embryoid body development. *Exp. Hematol.* **40**, 837–846 (2012).
- Zhang, L. *et al.* Modulation of TGF- β signaling by endoglin in murine hemangioblast development and primitive hematopoiesis. *Blood* **118**, 88–97 (2011).
- Borges, L. *et al.* A critical role for endoglin in the emergence of blood during embryonic development. *Blood* **119**, 5417–5428 (2012).
- Perlingeiro, R. C. Endoglin is required for hemangioblast and early hematopoietic development. *Development* **134**, 3041–3048 (2007).
- Kattman, S. J., Huber, T. L. & Keller, G. M. Multipotent flk-1 + cardiovascular progenitor cells give rise to the cardiomyocyte, endothelial, and vascular smooth muscle lineages. *Dev. Cell* **11**, 723–732 (2006).
- Huang, C. J., Tu, C. T., Hsiao, C. D., Hsieh, F. J. & Tsai, H. J. Germ-line transmission of a myocardium-specific GFP transgene reveals critical regulatory elements in the cardiac myosin light chain 2 promoter of zebrafish. *Dev. Dyn.* **228**, 30–40 (2003).
- Tian, H., Mythreya, K., Golzio, C., Katsanis, N. & Blobe, G. C. Endoglin mediates fibronectin/alpha5beta1 integrin and TGF-beta pathway crosstalk in endothelial cells. *EMBO J.* **31**, 3885–3900 (2012).
- Lints, T. J., Parsons, L. M., Hartley, L., Lyons, I. & Harvey, R. P. Nkx-2.5: a novel murine homeobox gene expressed in early heart progenitor cells and their myogenic descendants. *Development* **119**, 419–431 (1993).
- Kataoka, H. *et al.* Expressions of PDGF receptor alpha, c-Kit and Flk1 genes clustering in mouse chromosome 5 define distinct subsets of nascent mesodermal cells. *Dev. Growth Differ.* **39**, 729–740 (1997).
- Rasmussen, T. L. *et al.* ER71 directs mesodermal fate decisions during embryogenesis. *Development* **138**, 4801–4812 (2011).

17. Cohen, E. D., Tian, Y. & Morrisey, E. E. Wnt signaling: an essential regulator of cardiovascular differentiation, morphogenesis and progenitor self-renewal. *Development* **135**, 789–798 (2008).
18. Fuerer, C. & Nusse, R. Lentiviral vectors to probe and manipulate the Wnt signaling pathway. *PLoS ONE* **5**, e9370 (2010).
19. Moro, E. *et al.* In vivo Wnt signaling tracing through a transgenic biosensor fish reveals novel activity domains. *Dev. Biol.* **366**, 327–340 (2012).
20. Alt, A. *et al.* Structural and functional insights into endoglin ligand recognition and binding. *PLoS ONE* **7**, e29948 (2012).
21. Fuentealba, L. C. *et al.* Integrating patterning signals: Wnt/GSK3 regulates the duration of the BMP/Smad1 signal. *Cell* **131**, 980–993 (2007).
22. Morikawa, M. *et al.* ChIP-seq reveals cell type-specific binding patterns of BMP-specific Smads and a novel binding motif. *Nucleic Acids Res.* **39**, 8712–8727 (2011).
23. Takeuchi, J. K. *et al.* Chromatin remodelling complex dosage modulates transcription factor function in heart development. *Nat. Commun.* **2**, 187 (2011).
24. Xu, B. *et al.* Smad1 and its target gene Wif1 coordinate BMP and Wnt signaling activities to regulate fetal lung development. *Development* **138**, 925–935 (2011).
25. Fehling, H. J. *et al.* Tracking mesoderm induction and its specification to the hemangioblast during embryonic stem cell differentiation. *Development* **130**, 4217–4227 (2003).
26. Weiss, M. J., Keller, G. & Orkin, S. H. Novel insights into erythroid development revealed through in vitro differentiation of GATA-1 embryonic stem cells. *Genes Dev.* **8**, 1184–1197 (1994).
27. Drissen, R. *et al.* The erythroid phenotype of EKLF-null mice: defects in hemoglobin metabolism and membrane stability. *Mol. Cell Biol.* **25**, 5205–5214 (2005).
28. Shvidasani, R. A., Mayer, E. L. & Orkin, S. H. Absence of blood formation in mice lacking the T-cell leukaemia oncogene tal-1/SCL. *Nature* **373**, 432–434 (1995).
29. Saga, Y. *et al.* MesP1 is expressed in the heart precursor cells and required for the formation of a single heart tube. *Development* **126**, 3437–3447 (1999).
30. Cai, C. L. *et al.* Isl1 identifies a cardiac progenitor population that proliferates prior to differentiation and contributes a majority of cells to the heart. *Dev. Cell* **5**, 877–889 (2003).
31. Scortegagna, M., Morris, M. A., Oktay, Y., Bennett, M. & Garcia, J. A. The HIF family member EPAS1/HIF-2alpha is required for normal hematopoiesis in mice. *Blood* **102**, 1634–1640 (2003).
32. Ji, H. *et al.* Comprehensive methylome map of lineage commitment from hematopoietic progenitors. *Nature* **467**, 338–342 (2010).
33. Peng, G. *et al.* Spatial transcriptome for the molecular annotation of lineage fates and cell identity in mid-gastrula mouse embryo. *Dev. Cell* **36**, 681–697 (2016).
34. Stachura, D. L. *et al.* Clonal analysis of hematopoietic progenitor cells in the zebrafish. *Blood* **118**, 1274–1282 (2011).
35. Borges, L. *et al.* Expression levels of endoglin distinctively identify hematopoietic and endothelial progeny at different stages of yolk sac hematopoiesis. *Stem Cells* **31**, 1893–1901 (2013).
36. Hogan, B. L. M. Bone morphogenetic proteins: multifunctional regulators of vertebrate development. *Genes Dev.* **10**, 1580–1594 (1996).
37. Zafonte, B. T. *et al.* Smad1 expands the hemangioblast population within a limited developmental window. *Blood* **109**, 516–523 (2007).
38. Clevers, H. & Nusse, R. Wnt/beta-catenin signaling and disease. *Cell* **149**, 1192–1205 (2012).
39. Tarafdar, A., Dobbin, E., Corrigan, P., Freeburn, R. & Whealon, H. Canonical Wnt signaling promotes early hematopoietic progenitor formation and erythroid specification during embryonic stem cell differentiation. *PLoS ONE* **8**, e81030 (2013).
40. Tran, H. T., Sekkali, B., Van Imschoot, G., Janssens, S. & Vleminckx, K. Wnt/beta-catenin signaling is involved in the induction and maintenance of primitive hematopoiesis in the vertebrate embryo. *Proc. Natl Acad. Sci. USA* **107**, 16160–16165 (2010).
41. Jin, C. *et al.* Regulation of histone acetylation and nucleosome assembly by transcription factor JDP2. *Nat. Struct. Mol. Biol.* **13**, 331–338 (2006).
42. Ji, H. *et al.* Comprehensive methylome map of lineage commitment from hematopoietic progenitors. *Nature* **467**, 338–U120 (2010).
43. Maruyama, K. *et al.* The transcription factor Jdp2 controls bone homeostasis and antibacterial immunity by regulating osteoclast and neutrophil differentiation. *Immunity* **37**, 1024–1036 (2012).
44. Nojima, J. *et al.* Dual roles of smad proteins in the conversion from myoblasts to osteoblastic cells by bone morphogenetic proteins. *J. Biol. Chem.* **285**, 15577–15586 (2010).
45. Itou, J. *et al.* Migration of cardiomyocytes is essential for heart regeneration in zebrafish. *Development* **139**, 4133–4142 (2012).
46. Huber, T. L., Kouskoff, V., Fehling, H. J., Palis, J. & Keller, G. Haemangioblast commitment is initiated in the primitive streak of the mouse embryo. *Nature* **432**, 625–630 (2004).
47. Allinson, K. R., Carvalho, R. L., van den Brink, S., Mummery, C. L. & Arthur, H. M. Generation of a floxed allele of the mouse Endoglin gene. *Genesis* **45**, 391–395 (2007).
48. Hochdlinger, K., Yamada, Y., Beard, C. & Jaenisch, R. Ectopic expression of Oct-4 blocks progenitor-cell differentiation and causes dysplasia in epithelial tissues. *Cell* **121**, 465–477 (2005).
49. Langmead, B., Trapnell, C., Pop, M. & Salzberg, S. L. Ultrafast and memory-efficient alignment of short DNA sequences to the human genome. *Genome Biol.* **10**, R25 (2009).
50. Li, B. & Dewey, C. N. RSEM: accurate transcript quantification from RNA-Seq data with or without a reference genome. *BMC Bioinformatics* **12**, 323 (2011).
51. Boyer, L. A. *et al.* Core transcriptional regulatory circuitry in human embryonic stem cells. *Cell* **122**, 947–956 (2005).
52. Goecks, J., Nekrutenko, A. & Taylor, J. Galaxy: a comprehensive approach for supporting accessible, reproducible, and transparent computational research in the life sciences. *Genome Biol.* **11**, R86 (2010).
53. Langmead, B. & Salzberg, S. L. Fast gapped-read alignment with Bowtie 2. *Nat. Methods* **9**, 357–359 (2012).
54. Li, H. *et al.* The Sequence Alignment/Map format and SAMtools. *Bioinformatics* **25**, 2078–2079 (2009).
55. Zhang, Y. *et al.* Model-based analysis of ChIP-Seq (MACS). *Genome Biol.* **9**, R137 (2008).
56. Micsinai, M. *et al.* Picking ChIP-seq peak detectors for analyzing chromatin modification experiments. *Nucleic Acids Res.* **40**, e70 (2012).
57. Thorvaldsdottir, H., Robinson, J. T. & Mesirov, J. P. Integrative Genomics Viewer (IGV): high-performance genomics data visualization and exploration. *Brief Bioinform.* **14**, 178–192 (2013).
58. Ye, T. *et al.* seqMINER: an integrated ChIP-seq data interpretation platform. *Nucleic Acids Res.* **39**, e35 (2011).
59. Leng, N. *et al.* EBSeq: an empirical Bayes hierarchical model for inference in RNA-seq experiments. *Bioinformatics* **29**, 1035–1043 (2013).

Acknowledgements

This project was supported by NIH grants R01 HL085840 (R.C.R.P.), R01 AR055299 (R.C.R.P.), U01 HL100407R01 (R.C.R.P., D.J.G. and J.A.T.), R01 AR064195 (Y.K.), T32AR07612 (J.B.) and by a Regenerative Medicine Minnesota grant (A.M.). We are grateful to the UMN zebrafish core facility for fish maintenance and the Morgridge Regenerative Biology sequencing team for the RNA-Seq analyses. We thank Gordon Keller (University of Toronto) for kindly sharing Bry-GFP transgenic mice and reporter ES cells, Takenobu Katagiri (Saitama Medical University) for WT Smad1 construct and Helen Arthur (Newcastle University) for Eng-floxed mice.

Author contributions

J.B. designed and performed the research, analysed the data and wrote the manuscript; A.M. designed and performed the research, and analysed the data; N.T., N.K.N. and L.B. performed the research and analysed the data; S.S performed the bioinformatic analyses; R.S. and J.A.T. supervised the bioinformatic analyses; D.J.G. and Y.K. contributed with experimental design and interpretation of the data; R.C.R.P. contributed with experimental design and interpretation of the data, and wrote the manuscript.

Additional information

Supplementary Information accompanies this paper at <http://www.nature.com/naturecommunications>

Competing financial interests: The authors declare no competing financial interests.

Reprints and permission information is available online at <http://npg.nature.com/reprintsandpermissions/>

How to cite this article: Baik, J. *et al.* Endoglin integrates BMP and Wnt signalling to induce haematopoiesis through JDP2. *Nat. Commun.* **7**, 13101 doi: 10.1038/ncomms13101 (2016).

 This work is licensed under a Creative Commons Attribution 4.0 International License. The images or other third party material in this article are included in the article's Creative Commons license, unless indicated otherwise in the credit line; if the material is not included under the Creative Commons license, users will need to obtain permission from the license holder to reproduce the material. To view a copy of this license, visit <http://creativecommons.org/licenses/by/4.0/>